AIP | Applied Physics Letters

# Tensile deformation accommodation in microscopic metallic glasses via subnanocluster reconstructions

Ch. E. Lekka, A. Ibenskas, A. R. Yavari, and G. A. Evangelakis

Citation: Appl. Phys. Lett. **91**, 214103 (2007); doi: 10.1063/1.2816912
View online: http://dx.doi.org/10.1063/1.2816912
View Table of Contents: http://apl.aip.org/resource/1/APPLAB/v91/i21
Published by the American Institute of Physics.

## Related Articles

Large and electric field tunable superelasticity in BaTiO3 crystals predicted by an incremental domain switching criterion
Appl. Phys. Lett. 102, 092905 (2013)

Temperature and pressure dependent geometry optimization and elastic constant calculations for arbitrary symmetry crystals: Applications to MgSiO3 perovskites
J. Appl. Phys. 113, 103501 (2013)

Reduced losses in rolled Fe73.5Si15.5Nb3B7Cu1 nanocrystalline ribbon
J. Appl. Phys. 113, 17A306 (2013)

Design and fabrication of a bending rotation fatigue test rig for in situ electrochemical analysis during fatigue testing of NiTi shape memory alloy wires
Rev. Sci. Instrum. 84, 035102 (2013)

Exponential decay of shearing stress during jerky flows in a Zr-based bulk metallic glass
AIP Advances 3, 032105 (2013)

## Additional information on Appl. Phys. Lett.

Journal Homepage: http://apl.aip.org/
Journal Information: http://apl.aip.org/about/about_the_journal
Top downloads: http://apl.aip.org/features/most_downloaded
Information for Authors: http://apl.aip.org/authors

ADVERTISEMENT

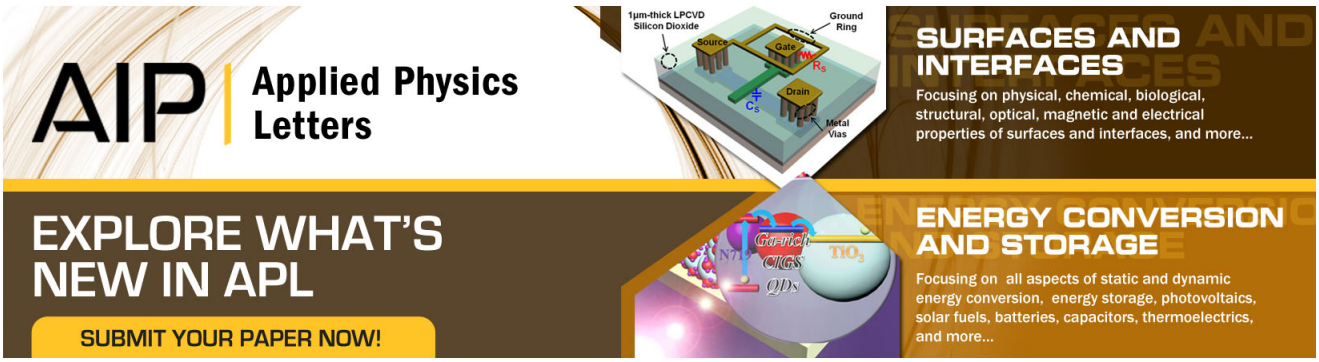

# Tensile deformation accommodation in microscopic metallic glasses via subnanocluster reconstructions

Ch. E. Lekka
*Department of Materials Science and Engineering, University of Ioannina, Ioannina 45110, Greece*

A. Ibenskas
*Department of Physics, University of Ioannina, Ioannina 45110, Greece*

A. R. Yavari
*SIMaP-LTPCM, Institut National Polytechnique de Grenoble, 38402 Saint Martin d'Heres, France*

G. A. Evangelakis[a)]
*Department of Physics, University of Ioannina, Ioannina 45110, Greece*

(Received 19 August 2007; accepted 1 November 2007; published online 21 November 2007)

We present results on the structure and the atomistic mechanisms for tensile deformation accommodation of the $Cu_{46}Zr_{54}$ microscopic metallic glass. At equilibrium, 23% of the atoms belong to tiny Cu-centered icosahedral clusters (Cu-ICO) and approximately 41% Zr centered slightly larger ICO-like clusters. Under deformation, the number of Cu-ICOs remains dynamically constant until yielding through a continuous cluster destruction-recreation process. Plastic deformation occurs homogeneously and is locally accommodated through the formation of rhombic dodecahedral clusters with significant ($\sim$2%) atomic density drop. These findings explain very recent experimental results demonstrating the fundamental differences of plastic deformation mechanisms between bulk metallic and microscopic glasses. © *2007 American Institute of Physics*. [DOI: 10.1063/1.2816912]

Metallic glasses (MGs) are amorphous solids exhibiting short and medium range order and fundamentally different deformation accommodation mechanisms from polycrystalline metals and alloys: plastic deformation occurs by interconnection of shear transformation zones[1–4] (STZs) instead of the motion of individual dislocations operating in polycrystalline solids. In the past, these zones have been assumed to be constituted of randomly closed packed atoms, e.g., in the form of small clusters, that respond spontaneously at various threshold applied stresses and reorganize their shapes through cooperative movements.[3,4] Bulk metallic glasses (BMGs) often exhibit macroscopic lack of ductility due to extreme localization of shear into thin bands of about 10 nm thick[5–7] referred to as shear bands that form when STZs percolate.[5–8] This in turn leads to shear softening, further shear localization, and early fracture, a phenomenon that has discouraged some of their applications as structural materials. Consequently, the ductilization of the MGs became one of the central points in the research in this field,[9–12] in conjunction with the efforts for building up MG composites that would exhibit plastic behavior while preserving high yielding point and toughness.[13] It came out that plastic deformation in macroscopic MGs not only occurs heterogeneously in shear bands but also the distance between individual shear bands observed in deformed metallic glasses depends on the specimen dimensions with interband distances being orders of magnitude larger than the shear band thicknesses of the order of 10 nm.[5]

In contrast, several very recent studies have shown that when the dimensions of the metallic glass are microscopic (of the order of less than 1 $\mu$m), plastic deformation becomes much more homogeneous[14] or fully homogeneous both in compression and tension.[8] Computer simulation techniques are well suited to gain insight of the plastic deformation behavior of metallic glasses with microscopic dimensions as reported here, with likely applications as structural materials in, for example, microelectronics and MEMS industries.

Focusing on the CuZr MGs, it is now accepted that (a) the microstructure of this MG contains small sized clusters basically of icosahedral-like order[15–18] (ICOs), (b) the presence of these nanoclusters influences seriously the mechanical response of MGs inducing ductility,[10,11,13] and (c) there are several indications that STZs are initiated at regions where certain types of such nanoclusters are located.[3,16,19]

We performed large-scale molecular dynamics simulations based on a tight binding in the second moment approximation (TBSMA) model adopted for the case of the $Cu_{46}Zr_{54}$ MG.[20,21] The glass was prepared in slab geometry with free surfaces from a liquid system of 128 000 atoms in the appropriate composition that was carefully cooled to room temperature at steps of 100 K, each of which lasted 15 ps, while the final configuration was aged for 0.5 ns. The structure of this system exhibited radial distribution functions typical of a glass; the inset of Fig. 1(a) depicts the partial radial distribution function (PRDF) for the Zr–Zr interactions at equilibrium (dashed line) and after yielding (solid line) upon tensile deformation of 24%. Clear manifestation of structural changes is visible by the alteration of the structure of the broad second peak. Figure 1(b) gives a close view of the development of this region upon successive deformations, while Fig. 1(c) gives the evolution of the initial (open circles) and the new (full circles) second peaks upon deformation, along with the strain-stress curve of the system (solid line). Besides the clear evidence of the structural changes, this picture reveals also that the material yields when these structural changes setup. Information on the sys-

a)Author to whom correspondence shoud be addressed. Electronic mail: gevagel@cc.uoi.gr

 

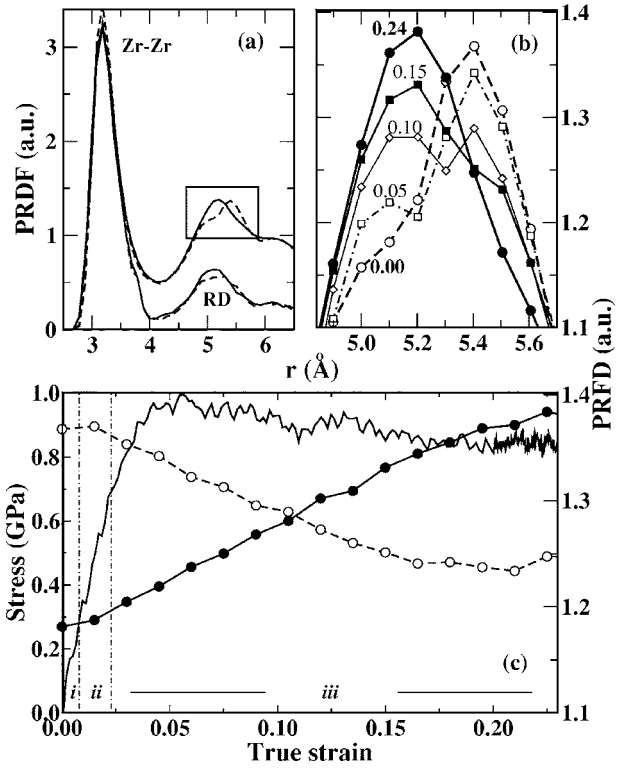


FIG. 1. (a) Partial radial distribution function (PRDF) for the Zr–Zr interactions along with the PRDF of the rhombic dodecahedron (RD) clusters before deformation (dashed line) and before failure (solid line). (b) The evolution of the 5.2 Å second neighbour peak upon deformation for strains 0.00 (open circles), 0.05 (open squares), 0.10 (open diamonds), 0.15 (full squares), and 0.24 (full circles). (c) Stress-strain curve (solid line) along with evolutions of the second PRDF peak at 5.4 Å (open circles) and the increase of the new one at 5.2 Å peak (full circles).

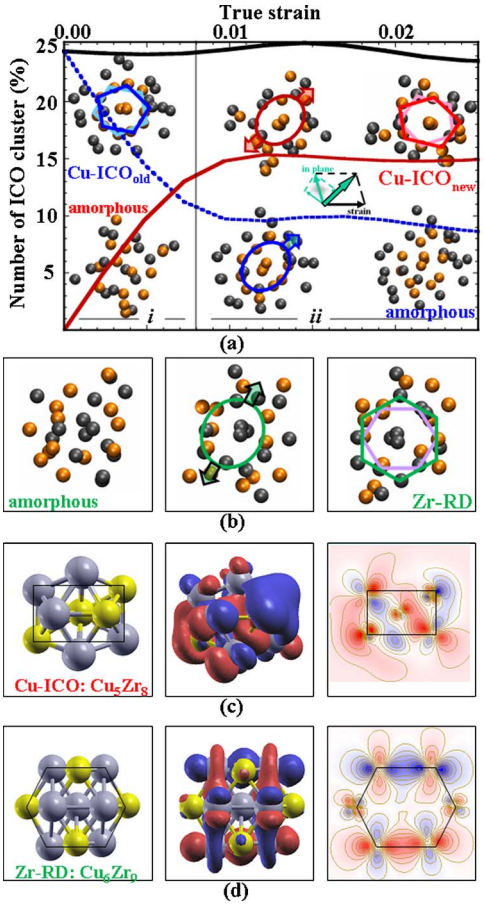


FIG. 2. (Color online) (a) Evolution of the number of Cu-ICO clusters: blue/dashed line stands for the old clusters, red/solid line for the new one, and black line corresponds to the total number of clusters. The processes of Cu-ICO destruction and creation are depicted in a sequence of snapshots. (b) Sequence of snapshots showing the transformation of the amorphous matrix to Zr-RD. (c) Calculated electronic charge distributions and isosurface maps of the HOMO state for the $Cu_5Zr_8$ and $Cu_6Zr_9$ clusters.

tem's microstructure was obtained with the use of common neighbour analysis (CNA).[22,23] It came out that 23% of the particles form very small (13 atoms) nearly perfect Cu-centered icosahedral (Cu-ICO) clusters, which may be touching and/or interpenetrating, 11% Cu-centered 13 atom bcc clusters and approximately 41% Zr centered slightly larger ICO-like clusters consisting of 14–17 atoms. The remaining 25% of the system's atoms belong to the surrounding amorphous matrix and involve local icosahedral fragments, distorted ICO clusters, and truncated octahedral clusters, which play the role of a "glue" for the nearly perfect clusters. The average composition of the ICO clusters was found to be $Cu_{5.4}Zr_{7.6}$, suggesting the presence of $Cu_5Zr_8$ and $Cu_6Zr_7$ clusters. These results are consistent with the independent calculation of the average atomic coordination number that exhibits a clear peak around 12–13, value that is indicative for ICO local order and in line with previous atomistic studies in which the presence of ICO-like clusters was evidenced and considered for the explanation of the short range order exhibited by these MGs.[3,19,22–25] Nevertheless, we anticipate that the size and also the number of these small clusters have to depend on the very high cooling rate imposed by the molecular dynamics time restrictions (the evaluation of the microstructure of a smaller system that was obtained by the application of ten times lower cooling rate, yielded denser system, and slightly larger clusters).

Upon tensile deformation the microstructure described above changes significantly. From the detailed structural analysis of the trajectory, we concluded to three remarkable findings [Fig. 2(a)]. (a) At every deformation step within the elastic region, some of the existing clusters (blue/dashed line) are destroyed and an almost equal number of new ones are created (red/solid line), resulting in dynamically constant total number of Cu-ICO clusters (black line). These processes are illustrated in the same figure in a sequence of snapshots. This dynamic situation persists until the strain of 0.008 is reached (marked as region i), while no statistically significant observable change was found in the surrounding amorphous matrix. (b) After this strain value and up to the yielding point 0.023 the rates of Cu-ICOs destruction and recreation drop rapidly and a number of small (around 15 atoms) Zr centered $Cu_6Zr_9$ rhombic dodecahedra (Zr-RD) clusters make their appearance at expense of the surrounding amorphous matrix (region ii). (c) After the yielding point, the applied deformation is accommodated mainly by the creation of RD clusters [region iii, Fig. 1(c)], while the destruction-creation process of the Cu-ICO clusters becomes gradually insignificant in this region and their number remains constant and almost equal to their initial value. It turns out, therefore, that in the latter region the amorphous matrix is progressively transformed into RDs [Fig. 2(b)], which, in fact, are precursors of the bcc-like structure, generating free volume and reducing the atomic density. We also note that under this severe plastic deformation, the clusters are forced gather and join between them, while the observed activity takes place

preferentially in a diagonal plane [indicated by arrows on the clusters and given in the inset of Fig. 2(a)] defined between the applied stress and the in-plane directions. Region ii coincides with the strain range in which the new peak at 5.12 Å in Fig. 1(b) appears, while this peak has its full development in the plastic deformation region that matches with region iii. It turns out, therefore, that the STZs are formed via the packing of the ICO-like clusters in region i, while the shear band formation process is initiated when these STZs associate together in region ii. The cluster destruction-recreation processes occurring in region i are in fact in line with Egami's concepts,[26–29] which attempt to describe the deformation of MGs through local atomic rearrangements that result in different coordinations and leading eventually in local alteration of the material's elastic modulus. In addition, the transitions taking place in region ii are in agreement with Miracle's efficient cluster packing model.[29,30] Taking into account the size of the simulated system, these processes refer to microscopic MGs. In the BMGs cases, much larger simulation cell is required in order to capture the transitions that can also occur in between the shear band regions that are usually orders of magnitudes larger and therefore the above description concerns only the very early stages of shear band formation.

It is worth noting that the identification of the RD clusters is not feasible by the CNA analysis mainly because most of them are distorted and/or truncated, thus yielding unclear CNA signatures. We overcame this difficulty by performing, at every applied strain in the regions ii and iii, selective local RDF calculations of the matrix (excluding the Cu-ICO regions) that were subsequently averaged and fitted to the corresponding RDFs of several candidate clusters. The outcome of this procedure yielded unequivocal evidence of the presence of the RD clusters [lower curve in Fig. 1(a)].

Taking into account the transferability limitations of the TBSMA models, in particular, when dealing with small-sized and/or low dimensional systems, we performed density functional theory (DFT) calculations[31] for the clusters found from the TBSMA simulations. It came out that the $Cu_5Zr_8$ Cu-ICO cluster is indeed energetically favored over the Zr centered ICO (−6.313 eV/atom compared to −6.255 eV/atom, respectively), while the Zr-RD is preferred against the Cu-RD for the $Cu_6Zr_9$ RDs clusters (−6.392 eV/atom against −6.371 eV/atom, respectively), in agreement with the TBSMA calculations. Figures 2(c) and 2(d) display the calculated electronic charge distributions and the isosurface maps of the highest occupied molecular orbital (HOMO) state for the Cu-ICO $Cu_5Zr_8$ and Zr-RD $Cu_6Zr_9$ clusters. It also came out that (a) in the Cu-ICO case, the Cu–Zr bonding is mainly through *d-d* orbital hybridizations, an effect that is less pronounced in the Zr-ICO case, resulting in stronger electronic overlap/bonding between the atoms. This result is in line with previous electronic structure calculations focused on the bonding type of this kind of MGs[8,15–19,21–25,32] and in agreement with the recent electronic rule for glasses formation.[32] (b) In the symmetric Zr-RD cluster, the Zr shell atoms form between them strong covalentlike *d-d* bonds and the central atoms exhibit metalliclike behavior. Although the above findings may depend on the relative atomic positions, the atomic bonding found remains practically unchanged and therefore these conclusions are nevertheless generic.

To conclude, we found that in the elastic region, the strain is accommodated via a continuous creation and destruction of Cu-ICO clusters, while the plastic deformation takes place homogeneously through the transformation of the amorphous matrix into small RD clusters assisted by the restructuring and the recombination of these subnanosized clusters. The latter process results in the generation of free volume[33] and leads to merged release of the local stresses leading eventually to the collective operation of the STZs. Taking into account the finite size of our simulation slab (the thickness is 13.3 nm, which is comparable to the thickness of a typical shear band ~10 nm), our predictions of homogeneous plastic deformation refer to microscopic MGs and explain recent experimental data.[8]

This work was supported by the MRTN-CT-2003-504692 project.

[1] A. S. Argon, Acta Metall. **27**, 47 (1979).
[2] F. Spaepen, Acta Metall. **25**, 407 (1977).
[3] C. A. Schuh and A. C. Lund, Nat. Mater. **2**, 449 (2003).
[4] A. R. Yavari, Nature (London) **439**, 405 (2006).
[5] R. D. Conner, W. L. Johnson, N. E. Paton, and W. D. Nix, J. Appl. Phys. **94**, 904 (2003).
[6] C. A. Schuh, A. C. Lund, and T. G. Nieh, Acta Mater. **52**, 5879 (2004).
[7] A. R. Yavari, J. J. Lewandowski, and J. Eckert, MRS Bull. **32**, 635 (2007).
[8] H. Guo, P. F. Yan, Y. B. Wang, Z. F. Zhang, J. Tan, M. L. Sui, and E. Ma, Nat. Mater. **6**, 73 (2007).
[9] K. Hajlaoui, B. Doisneau, A. R. Yavari, W. J. Botta, W. Zhang, G. Vaughan, A. Kvick, A. Inoue, and A. L. Greer, Mater. Sci. Eng., A **449-451**, 105 (2007).
[10] K. Hajlaoui, A. R. Yavari, J. Das, and G. Vaughan, J. Alloys Compd. **434-435**, 6 (2007).
[11] W. Zhang, C. Qin, X. Zhang, and A. Inoue, Mater. Sci. Eng., A **448-451**, 631 (2007).
[12] K. Hajlaoui, A. R. Yavari, A. LeMoulec, W. J. Botta, F. G. Vaughan, J. Das, A. L. Greer, and Å. Kvick, J. Non-Cryst. Solids **353**, 327 (2007).
[13] A. Inoue, W. Zhang, T. Tsurui, A. R. Yavari, and A. L. Greer, Philos. Mag. Lett. **85**, 221 (2005).
[14] Q. Zheng, S. Cheng, J. H. Strader, E. Ma, and J. Xu, Scr. Mater. **56**, 161 (2007).
[15] K. Saksl, H. Franz, P. Jóvári, K. Klementiev, E. Welter, A. Ehnes, J. Saida, A. Inoue, and J. Z. Jiang, Appl. Phys. Lett. **83**, 3924 (2003).
[16] D. V. Louzguine, M. Fukuhara, and A. Inoue, Acta Mater. **55**, 1009 (2007).
[17] L. Yang, H. J. Xia, Q. Wang, C. Dong, L. Y. Chen, X. Ou, J. F. Liu, J. Z. Jiang, K. Klementiev, K. Sakl, H. Franz, and J. R. Schneider, Appl. Phys. Lett. **88**, 241913 (2006).
[18] J. Saida, M. Kasai, E. Matsubara, and A. Inoue, Ann. Chim Sci. Mat. **27**, 77 (2002).
[19] A. C. Lund and C. A. Schuh, Acta Mater. **51**, 5399 (2003).
[20] D. G. Papageorgiou, A. Ibenskas, Ch. E. Lekka, and G. A. Evangelakis, Structural and Vibrational Properties of Deposited Cu or Zr surface adlayers on $Cu_{46}Zr_{54}$ Bulk Metallic Glass, J. Alloys Compd. (in press).
[21] G. Duan, X. Donghua, Q. Zhang, G. Zhang, T. Cagin, W. L. Johnson, and W. A. Goddard, Phys. Rev. B **71**, 224208 (2005).
[22] J. D. Honeycutt and H. C. Andersen, J. Phys. Chem. **91**, 4950 (1987).
[23] W. K. Luo, H. W. Sheng, F. M. Alamgir, J. M. Bai, J. H. He, and E. Ma, Phys. Rev. Lett. **92**, 145502 (2004).
[24] D. Srolovitz, V. Vitek, and T. Egami, Acta Metall. **31**, 335 (1983).
[25] M. L. Falk, Phys. Rev. B **60**, 7062 (1999).
[26] T. Egami, K. Maeda, and V. Vitek, Philos. Mag. A **41**, 883 (1980).
[27] T. Egami, Intermetallics **14**, 882 (2006).
[28] T. Tomida and T. Egami, Phys. Rev. B **48**, 3048 (1993).
[29] D. B. Miracle, T. Egami, K. M. Flores, and K. F. Kelton, MRS Bull. **32**, 629 (2007).
[30] D. B. Miracle, Nat. Mater. **3**, 697 (2004).
[31] D. Sanchez-Portal, P. Ordejon, E. Artacho, and J. M. Soler, Int. J. Quantum Chem. **65**, 453 (1997).
[32] M. Fukuhara, M. Takahashi, Y. Kawazoe, and A. Inoue, Appl. Phys. Lett. **90**, 073114 (2007).
[33] F. Spaepen, Scr. Mater. **54**, 363 (2006).